Int. J. Dynam. Control (2014) 2:198–209
DOI 10.1007/s40435-014-0085-6

Delay-margin design for the general class of single-delay retarded-type LTI systems

Rifat Sipahi

Received: 19 September 2013 / Revised: 27 February 2014 / Accepted: 11 March 2014 / Published online: 2 April 2014

Abstract For a given delay value $\bar{\tau}$, an approach is developed here to compute the iso-parameter settings of the general class of single-delay retarded-type LTI system such that this system can have a delay margin of precisely $\bar{\tau}$, and is thus guaranteed to be asymptotically stable for all positive delays less than $\bar{\tau}$.

Keywords Delay margin design · Stability · Linear delay system

1 Introduction

Time delays exist in many dynamical systems encountered in engineering, physics, biology, and economics [1–7]. As was extensively reported in the literature, when delays enter in a feedback loop in a system, e.g., via a closed-loop control architecture, the system may perform poorly and even become unstable. Many studies were hence devoted to the understanding of how delay affects the stability and closed-loop control of systems with delays [8–13].

Analyzing the stability of systems with delays can be challenging even for linear time invariant (LTI) systems. This is mainly due to the difficulties in managing, solving, handling some infinite dimensional eigenvalue problems arising from the analysis. One may choose to follow either one of the two research mainstreams to investigate stability, namely, those based on time-domain analysis [8,10,11,14], and those based on frequency domain [13–15]. These approaches have their respective superiorities, yet frequency domain techniques have been most preferred in cases when one wishes to analyze stability consistent with the Nyquist stability criterion, see, e.g., [12]. Along these lines, existing work is mainly focused on revealing the stability-instability decomposition of a given system with respect to a single or multiple system parameters. For instance, some studies [4,12,13,15–20] focus on revealing for which delay values τ an LTI system with single delay maintains its stability, whereas those in [4,12,13,21] explore the stability of the system with respect to system parameters. Moreover, the authors in [22] study the maximum delay margin achievable in a class of LTI systems with single delay, while in [4,13,16,23–29] the main objective is to reveal the "regions" in multiple-delay parameter space, where the LTI system is stable. The cited studies utilize various mathematical techniques to handle the difficulties inherently present in the stability analysis, all of which ultimately rely on two important fundamental theoretical results, namely, the continuity property of the arising eigenvalue problems in the parameter space [9], and the associated D-decomposition/τ-decomposition theorem [13,17].

Continuity property of system eigenvalues with respect to system parameters allows one to handle the stability analysis by focusing on whether or not these eigenvalues ever cross the imaginary axis of the complex plane. If they do, then the system may switch from stability to instability, or vice versa, depending on in which direction such eigenvalues move across the imaginary axis, with respect to the parameter of interest. This property then supports the D-decomposition/τ-decomposition theorem by which one should expect to find countably many regions in the parameter space, where in each region the system can possess only a finite number of unstable eigenvalues, N. Whenever $N = 0$ in a region, the system is

This research has been supported in part by the award from the National Science Foundation ECCS 0901442. A preliminary version of this work without proofs and details was presented at the American Control Conference 2012 held in Montreal, Canada.

R. Sipahi (✉)
Department of Mechanical and Industrial Engineering, Northeastern University, Boston, MA 02115, USA
e-mail: rifat@coe.neu.edu

stable for all the points in that region, and the boundaries that separate these regions are formed by some critical parameter values that impart imaginary-axis eigenvalues.

Several stability analysis techniques stemming from frequency domain, to a certain degree, can also be adapted for parametric analysis. For instance, one can relax a system parameter $p \in \mathbb{R}$, and investigate how the system stability along the delay axis $\tau(p) \geq 0$ is affected as the parameter varies in a range. This can be easily implemented within a stability analysis framework, and, as expected, would require a parameter sweep for p. While this approach can be satisfactory in some cases, it may not serve well for a general parametric design/synthesis problem in which one actually knows the precise amount of delay $\tilde{\tau} > 0$ in the control loop, and wishes to utilize this information to design the parameters $p(\tau)$ of the system. This is achieved as early as in 1960s on special classes of LTI systems with single delay by the work of Popov [12] pg. 437, as well as in [30] on a second-order system using the generalized Hermite-Biehler theorem. In such cases, one would desire to know the parameter settings of the system for which the system would maintain its stability for $\tau \in [0, \bar{\tau})$, where $\bar{\tau} > \tilde{\tau}$. That is, the control designer could select a delay value $\bar{\tau}$ such that $\bar{\tau} > \tilde{\tau}$, and reveal the iso-parameter curves $\bar{p}(\bar{\tau})$ along which the system at hand is in transition from stability to instability. The settings on these curves would hence guarantee the stability of the system for $0 \leq \tau < \bar{\tau}$.

To the best of our knowledge, for a given fixed $\bar{\tau}$ as described above, and also known as "delay margin" [15], a parameter design approach for the general LTI systems with a single delay has not been thoroughly investigated, and this article is devoted to address this design problem. Here, we focus on the retarded-type systems, however the presented approach could be expanded to handling neutral type and fractional type systems as well, paying attention to the peculiarities in eigenvalue behaviors of these types of systems [11,31].

In this article, we demonstrate that Rekasius transformation [32], which was utilized for various purposes [19,28,29,33–37], can also be used for the objective at hand, yet the implementation requires several non-trivial steps. Once these steps are tailored together, it becomes possible to reveal the iso-parameter curves of the LTI system at hand, where on the curves, the system is oscillatory at a frequency ω for the given delay value $\bar{\tau}$, and is stable $\forall \in [0, \bar{\tau})$. This inverse problem is indeed difficult to solve since one should find an approach to make sure that all the system eigenvalues except those on the imaginary axis $\mp j\omega$ are on the left-half plane, and at the same time, the delay value that places the eigenvalues on the imaginary axis is *precisely* at $\tau = \bar{\tau}$, while making sure that stability is maintained $\forall \in [0, \bar{\tau})$.

Notations used in the text are standard. We have $\mathbb{R}$ for the set of real numbers, and open left-half of complex plane $\mathbb{C}$ is represented by $\mathbb{C}_-$. We use $s \in \mathbb{C}$ for the Laplace variable; the delay is denoted by τ, while T stands for the parameter of the Rekasius transformation [32]. Arguments are omitted for easier reading when no confusion occurs.

2 Preliminaries

In this section, we first formulate the problem, and present some of the well-known fundamental concepts regarding the stability of the LTI system investigated.

2.1 Stability of a single-delay retarded-type LTI system

We start with the following general class of LTI systems with a single delay,

$$\frac{d}{dt}x(t) = Ax(t) + Bx(t-\tau), \tag{1}$$

where $x(t)$ is the state vector, A and B are state and control matrices, respectively, all with appropriate dimensions, and τ is the non-negative constant delay. The matrices A and B have numerical entries as well as parameters/controller gains $k_z \in \mathbb{R}$, $z = 1, \ldots, \bar{z}$.

The characteristic equation of the system in (1) is known to be in the following general form [19],

$$f(s; e^{-s\tau}) = \sum_{\ell=0}^{K} P_\ell(s, k_z) e^{-\ell s \tau} = 0, \tag{2}$$

where $\tau \geq 0$ is the delay, and P_ℓ are polynomials in terms of s. Notice that Eq. (2) is set up such that the polynomial $P_0(s)$ does not multiply any exponential functions and $P_0(s)$ has the largest power of s. This is because delay in (1) affects only the state $x(t-\tau)$. Systems with such property are called *retarded* class systems [13], which are encountered in many real-world problems [5,13,14].

For the stability analysis of the system in (1), the previous work [4,5,12,16,18,19,38] mainly focused on characterizing the delay parameter space $\tau \geq 0$ as stabilizing and destabilizing intervals. These studies are concerned with the *analysis* of the delay parameter space, "given" the parametric values $k_z = k_z^*$. For this, the analysis starts with detecting the stability transitions of the roots of (2) in delay parameter space. The key knowledge used in all the studies is the continuity property of these roots on $\mathbb{C}$ [9], which states that stability transitions may occur only when at least one root of (2) is on the imaginary axis at $s = j\omega$ for some τ^*, where the frequency ω is non-negative without loss of generality, [12,16]. In other words, at the stability transitions of the system, the following equation must hold,

$$f(j\omega; e^{-j\omega\tau}) = \sum_{\ell=0}^{K} P_\ell(j\omega, k_z) e^{-j\ell\omega\tau} = 0. \tag{3}$$

2.2 Rekasius substitution and some properties of stability transitions

We present the remainder of the section for k_z given. Among many techniques and mathematically elegant manipulations utilized in the stability analysis of (1), one of them, a transformation proposed by Z. V. Rekasius [32], attracted further attention (see cited studies above), which we will also utilize in the Main Results section. The transformation given by

$$e^{-j\omega\tau} := \frac{1 - jT\omega}{1 + jT\omega}, \tag{4}$$

where $T \in \mathbb{R}$, suggests that all the exponential terms in (2) are to be replaced by the right-hand side of (4). Note that this transformation is exact, and should not be confused with Padé approximation.

With the substitution of (4) into (2), and after removing the fractions by expansion, which does not bring any artificial $s = j\omega$ roots, one obtains a new characteristic equation,

$$g(j\omega; T) = (1 + jT\omega)^K f\left(j\omega; e^{-j\omega\tau} = \frac{1 - jT\omega}{1 + jT\omega}\right) = 0, \tag{5}$$

which is algebraic and parametric in T. While performing the above conversion from (3) to (5), no approximation is imposed, and accuracy is not lost since the infinite dimensional nature of the problem is preserved in the algebraic polynomial (5) with the help of the additional parameter $T \in \mathbb{R}$ [19,32], termed the pseudo-delay [39] and core generators [29]. Moreover, as established earlier [32], the substitution (4) is valid and exact so long as τ complies with

$$\tau_q = \frac{2}{\omega}[\arctan(\omega T) \mp q\pi], \quad q = 0, 1, 2, \ldots, \infty, \tag{6}$$

which can be easily derived from (4). That is, the imaginary roots of (2) and (5) are one to one identical [29]. Yet, extracting these roots from (5) is more practical owing to its algebraic form.

Equation (6) indicates that for some T and ω satisfying (5) at $s = j\omega$, there exists infinitely many τ solutions found from (6) that also satisfy (2) at $s = j\omega$, see [19,29]. In other words, each (T, ω) pair that satisfies (5) for $s = j\omega$ maps to points $(\tau_0, \tau_1, \ldots, \tau_q, \ldots)$ found from (6). These points mark the delay parameter space, bisecting it into intervals, where in each interval the system is either stable or unstable. These properties comply with the very fundamentals of the stability properties of retarded class systems based on τ-decomposition principle [12,13,17].

Following from the above discussions, one can formalize stability-transition properties of the system as follows. The crossing frequency set of (1) is defined as

$$\Omega = \{\omega_1, \ldots, \omega_m\}, \tag{7}$$

with respective T values,

$$\Upsilon = \{T_1, \ldots, T_m\}, \tag{8}$$

and corresponding delay values are found, using (7) and (8), as

$$\tau_{k,q} = \frac{2}{\omega_k}[\arctan(\omega_k T_k) \mp q\pi], \quad k = 1, \ldots, m, \quad q = 0, 1, 2, \ldots, \infty, \tag{9}$$

where $\tau_{k,0}$ is the *smallest positive delay value*, see [19][29].

Remark 1 Notice that the approaches described in the literature including those stemming from Rekasius transformation are implemented to calculate the stable-unstable regions of the LTI system along the delay axis, see cited studies above. That is, calculation of the delay values is an "end result" in these approaches. Nevertheless, solving the reverse problem, that is, synthesizing the stability/instability decomposition of the delay axis with k_z being the end-result of the design is not straightforward, as we detail in the following section.

2.3 Delay margin and number of crossings

The delay margin $\bar{\tau}$ of the system (1) is the smallest positive delay value at which the delay-free stable system transitions to instability [15]. That is, it is required that the system is stable when free of delays ($\tau = 0$), and in that case, the delay margin is defined as $\bar{\tau} = \min_k(\tau_{k,0})$.

One critical point here is the number of crossings m. If $m = 1$, it is easy to detect the delay margin $\bar{\tau} = \tau_{k,0}$; however when $m > 1$, then the delay margin is the smallest of $\tau_{k,0}$, $k = 1, \ldots, m$. In the next section, this will play an important role in designing the system parameters for a given delay margin.

The number m can be determined in various ways [38], one being borrowed here from [18]:

Lemma 1 [18] *The number of imaginary axis crossings m can be at most* $2n^2$*, where n is the dimension of* (1).

From the work [18], which was also surveyed in [38], one defines

$$\Gamma_0 = I \otimes I, \quad \Gamma_1 = I \otimes A - A \otimes I, \quad \Gamma_2 = B \otimes B - A \otimes A, \tag{10}$$

with which the following matrix made of $n^2 \times n^2$ block matrices is computed

$$\Pi = \begin{pmatrix} 0 & \Gamma_0 \\ -\Lambda_2 & -\Lambda_1 \end{pmatrix}, \tag{11}$$

where $\Lambda_1 = \Gamma_0^{-1}\Gamma_1$ and $\Lambda_2 = \Gamma_0^{-1}\Gamma_2$.

Lemma 2 [18] *Let* $S = \{\lambda_1(\Pi), \ldots, \lambda_{2n^2}(\Pi)\}$. *Then it holds that* $\Omega \subseteq S$.

In other words, to find the number of crossings[1] m, one can first compute the eigenvalues of matrix Π, and next follow [18] to verify which eigenvalues are in the set Ω.

Further details regarding the detection of the delay values $\tau_{k,q}$ in (9). can be found in [5,13,38] and the cited studies in the previous section regarding analyzing the stability-instability composition of the delay axis for fixed k_z.

3 Main results

In this section, the objective is to reveal an approach by which one can design the parameters $k_z \in \mathbb{R}$ in (2) such that the system represented by (2) is stable for $\tau \in [0, \bar{\tau})$, given $\bar{\tau}$. Note that we restrict this design to synthesizing the delay axis only for the delay margin $\bar{\tau}$, and future work will be focused on designing multiple stability intervals along the delay axis.

As per problem setup, the system for $\tau = \bar{\tau}$ must have eigenvalues at $s = j\omega^*$, and hence it is necessary that the following equation holds,

$$f(j\omega^*; e^{-j\omega^*\bar{\tau}}, k_z) = \sum_{\ell=0}^{K} P_\ell(j\omega^*, k_z) e^{-\ell\, j\omega^*\, \bar{\tau}} = 0. \quad (12)$$

To be able to solve the above equation in order to compute the iso-parameter curves for a given $\tau = \bar{\tau} > 0$, one should solve (12) for $\omega^* \in \mathbb{R}$ and $k_z \in \mathbb{R}$, however this is not an easy task for various reasons:

(a) Equation (12) is transcendental with infinitely many solutions $(\omega^*, k_1, \ldots, k_z, \ldots, k_{\bar{z}})$, whether or not they all lie in real domain,
(b) One should find a specific solution of $\omega^* \in \mathbb{R}$ and $k_z \in \mathbb{R}$ such the infinitely many roots of (2) for $\tau = \bar{\tau}$ have negative real parts, except those at $s = j\omega^*$.
(c) A feasible solution of parameters k_z guaranteeing the desired delay margin $\bar{\tau}$ may not exist.
(d) The system may have multiple crossings, $m > 1$, making the design process complicated.

In the following, we propose an approach by which we can determine whether or not the iso-parameter curves exist, and if they exist, we can detect these curves.

3.1 Derivation of design rules

The proposed design procedure is constructed based on the following logic line:

[1] Note that Lemma 1 considers both positive and negative values of ω. Hence, the number of positive ω solutions is at most n^2, since the roots of the characteristic equation must be symmetric, see also [38] for discussions.

Given the known delay value $\tau = \tilde{\tau}$ in the control loop in (1), the control designer selects a finite delay $\bar{\tau}$, where $\bar{\tau} > \tilde{\tau}$, and calculates the set of system parameters lying on some iso-parameter curves corresponding to system's stability margin $\bar{\tau}$ such that the same system is for sure guaranteed to be asymptotically stable $\forall \tau \in [0, \tilde{\tau}]$.

Let us first identify the necessary rules that need to be respected for a feasible solution to exist:

Rule 1: Since it is required that the system is stable for $\tau = 0$, one needs to guarantee the stability of the delay-free system. This requires that $A + B$ is a Hurwitz matrix, or equivalently, the roots of $f(s; 1) = 0$ all lie in $\mathbb{C}_-$. This part of the analysis can be trivially established using the Routh-Hurwitz stability criterion [40].

Since we guarantee the stability of the delay-free system, we know that the system cannot have an eigenvalue at $s = 0$ for any finite delay in $\mathbb{R}_+$ [41]. Moreover, without loss of generality, we can focus only on the positive real axis of the ω parameter, thus we have $\omega > 0$ in the rest of the text.

Lemma 3 *Given $\bar{\tau}$, the solution ω^* of (12) satisfies the condition $0 \leq \omega^* < 2\pi/\bar{\tau}$.*

Proof Notice that the positive delay solutions satisfying (2) for ω^* when arranged in increasing order on the delay axis should have the following properties. First of all, the minimum positive delay solution, i.e., the positive delay value closest to the origin of the delay axis, must be the predetermined value $\bar{\tau}$. Moreover, for delay $\bar{\tau}$ to really be the minimum positive delay, it is necessary that the delay value preceding $\bar{\tau}$ is negative, which requires, from the inspection of (6), that the inequality $\bar{\tau} - \frac{2\pi}{\omega^*} < 0$ holds, which proves the lemma. □

Rule 2: In light of Lemma 3, it is necessary that $0 < \omega^* < 2\pi/\bar{\tau}$ holds.

Lemma 4 *Let $\phi = \omega^* T \in \mathbb{R}$. The minimum positive delay $\bar{\tau}$ can be formulated as follows:*

$$\bar{\tau} = \begin{cases} \frac{2}{\omega^*} \arctan(\phi), & \text{where } \phi > 0, \\ \frac{2}{\omega^*}[\arctan(\phi) + \pi], & \text{where } \phi < 0. \end{cases} \quad (13)$$

Proof Use (6) to calculate the minimum positive delay value as follows. If $\phi > 0$, then $\pi/2 > \arctan(\phi) > 0$, and $q = 0$ in order to calculate the minimum positive delay value. But if $\phi < 0$, then $-\pi/2 < \arctan(\phi) < 0$. This requires to set $q = 1$ so that the delay value can still be made minimum and positive. Other values of q render positive delays but violate the minimum positivity condition, can hence be ignored. □

Remark 2 Notice that $\phi = 0$ is ignored here as it requires that the characteristic equation has an imaginary root $s = j\omega^*$ for either $\omega^* = 0$, or $T = 0$. Notice from [19,32] that $T = 0$ and $\tau = 0$ give rise to identical characteristic equations as

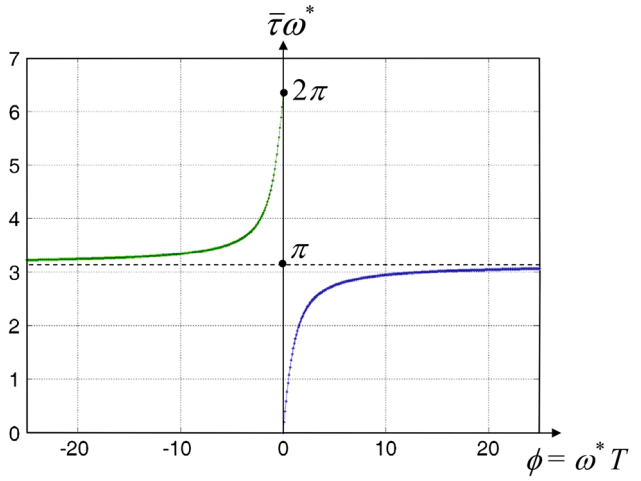

Fig. 1 The curve $\bar{\tau}\omega^*$ as a function of $\phi = \omega^* T$. Here $\bar{\tau}$ is known and fixed

a special case. As per Rule 1, since the delay-free system is asymptotically stable, having imaginary roots $s = j\omega^*$ for $T = 0$ is not possible. Furthermore, it is known from [41] that $\omega \to 0$ as $\tau \to +\infty$, which does not comply with the assumption that $\bar{\tau}$ is finite.

Rule 3: As per the above discussions, for a given ϕ, the frequency ω^* is calculated from (13) as

$$\omega^* = \frac{2}{\bar{\tau}}\left(\arctan(\phi) - \frac{(signum(\phi) - 1)\pi}{2}\right), \quad \phi \neq 0. \tag{14}$$

Equation (14) can be used to visualize the function $\bar{\tau}\omega^*$, see Fig. 1, which shows that $\bar{\tau}\omega^*$ is upper/lower bounded.[2] As can be seen in the figure, the curve $\bar{\tau}\omega^*$ has some features. First of all, it scales proportionally with ω^*; it monotonically increases as ϕ varies from $-\infty$ to $+\infty$, except a drop at $\phi = 0$, which is ignored as per Remark 2; given the closed-loop delay $\tilde{\tau}$ and depending on the value of ω^*, one can find a range of ϕ such that $\bar{\tau}$ can be designed to be larger than $\tilde{\tau}$; due to monotonicity properties and that ω^* is only a scaling parameter, for a given ω_0 the constant line $\tilde{\tau}\omega_0$ intersects the curve $\bar{\tau}\omega^*$ at one and only one point, except when $|\phi| \to \infty$. Nevertheless, it is easy to confirm from (14) that one obtains the same numerical value for both $\phi \to +\infty$ and $\phi \to -\infty$, which is π.

In light of Rule 3, it makes sense to propose the following approach to compute the iso-parameter curves. Let ϕ be the sweep parameter[3] in an interval $\phi \in [\underline{\phi}, \overline{\phi}]$. Then, for a given $\phi \in [\underline{\phi}, \overline{\phi}]$, one can compute from (4) the following

$$e^{-j\omega^*\bar{\tau}} = \frac{1 - j\phi}{1 + j\phi}, \tag{15}$$

which suggests that all $e^{-j\omega^*\bar{\tau}}$ terms in (12) can be replaced by the complex number on the right hand side of (15). With this replacement, the characteristic equation to be studied becomes less complicated since the exponential terms are removed,[4]

$$f\left(j\omega^*; \frac{1-j\phi}{1+j\phi}, k_z\right) = \sum_{\ell=0}^{K} P_\ell(j\omega^*, k_z)\left(\frac{1-j\phi}{1+j\phi}\right)^\ell = 0, \tag{16}$$

which is a polynomial with complex coefficients and in terms of ω^* and system parameters k_z. Moreover, notice that the value of ω^* is dependent on ϕ and is known as per (14). Therefore, by dropping the arguments that are numerically known, and leaving only the design parameters as arguments, we have

$$f(k_z) = f_\Re(k_z) + j f_\Im(k_z) = 0, \tag{17}$$

which can hold if and only if $f_\Re = 0$ and $f_\Im = 0$. That is, in order to find the iso-parameter curves in k_z domain, one should study the common solutions of the following two polynomials with real coefficients,

$$f_\Re(k_z) = 0, \tag{18}$$
$$f_\Im(k_z) = 0. \tag{19}$$

Rule 4: Notice that the procedure described above must be followed by the consideration of the number of crossings of the system, m. For this, once the common solutions of (18)–(19) are found, for each solution point k_z, one should revisit Lemma 2 to perform the following tests in order to verify whether or not k_z is a feasible solution[5]:

(a) Find the value m.
(a1) If $m = 1$, then proceed to step (b),
(a2) If $m > 1$, then compute $\tau_{k,0}$ from (9),
(a2.1) If $\bar{\tau} \leq \min_{k=1\ldots m} \tau_{k,0}$, then $\bar{\tau}$ is indeed the smallest possible delay causing a loss of instability, as desired in the design process, and hence one proceeds to step (b);

[2] The fact that $\tau\omega \in [0, 2\pi]$ was previously used for "analysis purposes", within the 'Building Block' concept in [41].

[3] This is analogous to "frequency sweeping" ideas introduced in [42], except that the frequency ω here is scaled by the pseudo-delay parameter T. This may also resemble the Building Block concept [41], yet in the previous work, $\tau\omega$ is the sweep parameter, and the delay margin $\bar{\tau}$ is to be calculated as an end result but is not fixed in the problem formulation.

[4] This is possible since the delay $\bar{\tau}$, ω^*, and the "scaled" frequency ϕ are numerically known. We introduced this idea for a different purpose in [28] mainly for taking 2D cross-sectional views of stability maps of LTI systems with more than three independent delays.

[5] Note that by design we are enforcing one crossing in the system, hence $m \neq 0$.

(a2.2) If $\bar{\tau} > \min_{k=1\ldots m} \tau_{k,0}$, then this means there exists a different and smaller positive delay value that initiates a loss of instability, and hence one should proceed to step (c);
(b) The value k_z is feasible.
(c) The value k_z is not feasible.

Corollary 1 *For a given ϕ, a point on the iso-parameter hypersurfaces in k_z parameter space exists if and only if the polynomials in (18)–(19) have a common root; and this root satisfies Rules 1–2 as well as either one of the following conditions:*

(a) $m = 1$; or
(b) $m > 1$ and $\bar{\tau} \leq \min_{k=1\ldots m} \tau_{k,0}$ holds.

Proof First step of the proof follows from the fact that a common root k_z of (18)–(19) is also a root of the original characteristic Eq. (12), as per the properties of Rekasius substitution [29]. Moreover, since Rule 1 holds, the system is stable for $\tau = 0$, and since Rule 2 holds, the crossing ω^* occurs at $\tau = \bar{\tau}$, which is the smallest positive delay value. Since ω^* is enforced by design, we have $m \geq 1$. If $m = 1$, then this is the enforced crossing, and there are no other imaginary axis crossings, and thus k_z is on the iso-parameter curve (item (a)). However, if $m > 1$ for a k_z value satisfying (18)–(19), then it is necessary to check whether or not any additional crossings violate the intended delay margin design. As explained above, as long as additional crossings occur at delay values larger than $\bar{\tau}$, the intended design will be successful (item (b)). Conversely, if there are more than one crossing, $m > 1$, with at least one delay value less than $\bar{\tau}$, then the intended delay margin design fails, similar to when Rule 2 does not hold. If Rule 1 does not hold, then the system does not have a delay margin by definition, and since the Rekasius substitution is a two-way condition [29]; the design fails if (18)–(19) do not have common k_z roots, which would imply that a solution k_z does not exist satisfying the original characteristic Eq. (12). □

Notice that equations in (18)–(19) are multi-variate polynomials, and in general, for more than three independent parameters, the complete solution set may not be easily obtained. Nevertheless, the analytical form of these polynomials can be used to perform various parametric studies, for instance, for designing the PI gains controlling a plant with transport delay [30]. Moreover, if one wishes to explore the parametric variations in k_z starting from a known initial point $k_z = k_{z,0}$, then it would be possible to explore the common solutions of the hypersurfaces (18)–(19) by implementing a continuation algorithm. These types of increased-dimension issues are inevitable, and arise in various multi-parameter problems, where parametric sweeping is the only choice; see a discussion on this in [26,43].

In the case when there are less than three independent variables, $z < 3$, more tractable results are possible as explained next:

3.1.1 One independent variable k

A single parameter design is the simplest case, however it carries some inherent challenges since there is only one free parameter that should satisfy (18)–(19) simultaneously. Due to this reason, an explicit solution of k is not possible in general, and one should use graphics to determine the common solutions, as detailed next.

In the case of a single variable k, one needs to find the common solutions in (18)–(19) for a given ϕ, but this is not easy since ω^* is dependent on ϕ, see (14). That is, we have $\omega^*(\phi)$. One way to tackle this problem is to solve k from (18)–(19), and form an 'error' function as follows. Let k solved from (18) and (19) be denoted respectively by $k_{\Re}$ and $k_{\Im}$. Then the error function is formulated only by a function of ϕ as follows,

$$e(\phi) = k_{\Re} - k_{\Im}, \tag{20}$$

zeros of which are the candidate solutions $\tilde{\phi}$ found graphically and via nonlinear solvers. Using the candidate solutions $\tilde{\phi}$, one can compute ω^* using (14), and subsequently the value of $k = k_{\Re} = k_{\Im}$. If these candidate solutions satisfy Rules 1–2 and Rules 4, then they lie on the iso-parameter curves, as per Corollary 1.

Notice that the above approach requires to plot the error function $e(\phi)$ with respect to ϕ, and to use a nonlinear solver to compute the zero crossings of the error function along the ϕ-axis.

3.1.2 Two independent variables k_1 and k_2

In some problems, it is possible to solve k_1 and k_2 explicitly from (18)–(19), which would yield a solution in the following form

$$k_1 = k_1(\phi, \omega^*), \tag{21}$$
$$k_2 = k_2(\phi, \omega^*), \tag{22}$$

in which one sweeps the single parameter ϕ in connection with (14) in order to obtain the candidate points, which can then be refined in Corollary 1, in order to reveal the iso-parameter curves in an automated way. However, in general, simultaneous solution of (18)–(19) may not be possible since

the polynomials are in the following form

$$f_{\Re}(k_1, k_2) = \sum_{\ell_1}^{L_1} \gamma_{\ell_1}(k_1) k_2^{\ell_1} = 0, \tag{23}$$

$$f_{\Im}(k_1, k_2) = \sum_{\ell_2}^{L_2} \gamma_{\ell_2}(k_1) k_2^{\ell_2} = 0, \tag{24}$$

where L_1 and L_2 are integers, and γ_{ℓ_1} and γ_{ℓ_2} are polynomials only in terms of k_1. In such cases, the common solutions of (23)–(24) can be found by the implementation of resultant theory [44]. For this, one constructs the Sylvester's matrix using the coefficients $\gamma_{\ell_1}(k_1)$ and $\gamma_{\ell_2}(k_1)$. That is, the entries of the Sylvester's matrix are in terms of only k_1. According to the resultant theory, if the polynomials (23)–(24) have a common solution (k_1^*, k_2^*), then the Sylvester's matrix is singular, however the converse is not always true. To utilize this property, one can compute the determinant of the Sylvester's matrix, and study the zeros of this determinant, which depend on only k_1. The zeros $\tilde{k}_1$ of the determinant are candidate solutions. Each candidate $k_1 = \tilde{k}_1$ is substituted into (23), in order to solve for candidate $k_2 = \tilde{k}_2$ roots. One then tests whether or not any of the pairs $(\tilde{k}_1, \tilde{k}_2)$ satisfy (24). Those satisfying (23)–(24) are the common solutions (k_1^*, k_2^*) that we are after. These solutions are then further processed in Corollary 1 in order to detect the iso-parameter settings.

3.2 Case study 1

Let us investigate the scalar single-delay LTI dynamics with the following characteristic equation,

$$f(s; e^{-\bar{\tau}s}) = s + a + be^{-\bar{\tau}s} = 0, \tag{25}$$

where $\bar{\tau} > 0$ is given.

3.2.1 a is fixed, and b is the only free parameter

In this case, the equations corresponding to (18)–(19) are computed as follows,

$$f_{\Re}(b) := -\omega^*\phi + a + b = 0, \tag{26}$$

$$f_{\Im}(b) := \omega^* + \phi(a - b) = 0. \tag{27}$$

From (26) we solve $b_1 := b$, and with the fact that $\phi \neq 0$ as per Remark 2, we can solve $b_2 := b$ from (27),

$$b_1 = \phi\omega^* - a, \tag{28}$$

$$b_2 = \frac{\omega^* + a\phi}{\phi}. \tag{29}$$

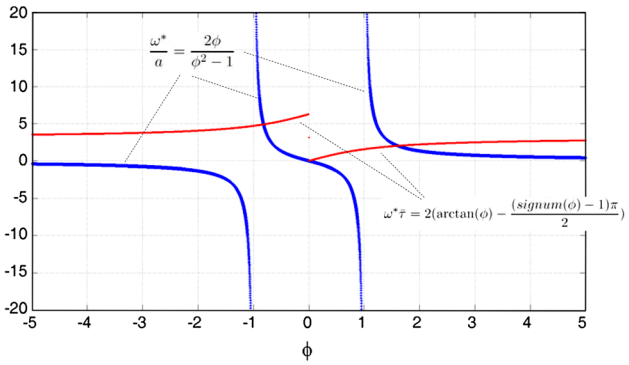

Fig. 2 Proof of Lemma 5: Comparison of $\frac{\omega^*}{a}$ with $\omega^*\bar{\tau}$

Using the two equations above, the error function can be organized as follows

$$e(\phi) := b_1 - b_2 = \frac{\omega^*\phi^2 - 2a\phi - \omega^*}{\phi}, \tag{30}$$

which must be solved for its zeros.

Lemma 5 *For a given a and $\bar{\tau}$, the system represented by the characteristic equation in (25) can be made stable for $\tau \in [0, \bar{\tau})$ at most by two b values.*

Proof Since ω^* is always finite as the system at hand is of retarded type [13], we have $e(\phi) \neq 0$ for $\phi \to \infty$, and hence we can focus on studying the zeros of the numerator of (30), which can be organized as

$$\omega^* = \frac{2a\phi}{\phi^2 - 1}. \tag{31}$$

The above equation must hold under the constraint (14) describing the dependency of ω^* on ϕ, see also Fig. 1. Moreover, for any given a, the right hand side of (31) is monotonically decreasing in ϕ either from zero to negative infinity, or from positive infinity to negative infinity, or from positive infinity to zero, and this function is negative for $\phi < -1$ and $\phi \in (0, +1)$ where it cannot intersect with the function ω^*, which is always positive, see Fig. 2. Furthermore, ω^* function is also a monotonic function, where it is increasing from $\pi/\bar{\tau}$ to $2\pi/\bar{\tau}$ as ϕ changes from $-\infty$ to zero, and increasing from zero to $\pi/\bar{\tau}$ as ϕ changes from zero to $+\infty$. Consequently, since $\phi = 0$ is not considered in the analysis, we have that the two curves on both sides of the equation sign in (31) can intersect at most two times. □

3.2.2 a and b are free parameters

Lemma 6 *The system represented by the characteristic equation in (25) is stable for $\tau \in [0, \bar{\tau})$ if and only if the following conditions simultaneously hold:*

(i) $a + b > 0$;

(ii) The parameter pair (a, b) lies on the contours parameterized by ϕ,

$$a(\phi, \bar{\tau}) = \frac{(\phi^2 - 1)(\arctan(\phi) - (signum(\phi) - 1)\pi/2)}{\bar{\tau}\phi}, \tag{32}$$

$$b(\phi, \bar{\tau}) = \frac{(\phi^2 + 1)(\arctan(\phi) - (signum(\phi) - 1)\pi/2)}{\bar{\tau}\phi}. \tag{33}$$

Proof Item (i) follows from Rule 1. Furthermore, following the proposed approach above, one can find the parametric curves $a(\phi, \bar{\tau})$ and $b(\phi, \bar{\tau})$ as

$$a(\phi, \bar{\tau}) = \frac{\omega^*(\phi)(\phi^2 - 1)}{2\phi}, \tag{34}$$

$$b(\phi, \bar{\tau}) = \frac{\omega^*(\phi)(\phi^2 + 1)}{2\phi}, \tag{35}$$

into which $\omega^*(\phi)$ in (14) can be plugged to get (32)–(33). Since (14) is used to plug in ω^*, Rule 2 is automatically satisfied. Moreover, following [20] it is easy to show that the system at hand can have maximum of one crossing $m = 1$, and hence the computed (a, b) pairs are feasible as per Corollary 1.

In light of item (i) in Lemma 6, using (34)–(35), we have

$$a + b = \phi\omega^*(\phi) > 0, \tag{36}$$

from which we conclude that $\phi > 0$ must hold, since $\omega^*(\phi) > 0$ as per Rule 2. This result along with the fact that $m = 1$ indicates that there is always a feasible (a, b) pair $\forall\phi > 0$.

Corollary 2 *The parameters a and b that make the system represented by (25) stable for $\tau \in [0, \bar{\tau})$ are unbounded in positive real domain.*

Proof Proof follows from the fact that, since ω^* is always upper bounded as per Rule 2, the term ϕ^2 dominates the numerator of (32)–(33), and that a feasible (a, b) pair always exists $\forall\phi > 0$. □

Lemma 7 *There exists at least one (a, b) pair for which the finite delay margin $\bar{\tau}$ of the system represented by (25) can be made arbitrarily large.*

Proof It follows that Eqs. (32)–(33) are inversely proportional to $\bar{\tau}$, and thus, for arbitrarily large $\bar{\tau}$ values, feasible but arbitrarily small values of a and b exist, in support of Corollary 2. □

3.3 Case study 2

Consider the problem studied in [30], where an open loop plant with transfer function

$$G(s) = K\frac{e^{-\tau s}}{\alpha s + 1},$$

is controlled by a PI controller of the form

$$C(s) = k_p + \frac{k_i}{s},$$

with a unity negative feedback, and the constant delay in the plant is known to be fixed at $\tau = \tilde{\tau}$. Using the approach described above, we can calculate the PI gains (k_p, k_i) for which the closed-loop system can be made oscillatory, that is, $\bar{\tau} = \tilde{\tau}$. Without loss of generality, we take $K = 1$, and investigate the case of stable open-loop system, i.e., $\alpha > 0$.

The characteristic equation of the system for $\tau = \bar{\tau} = \tilde{\tau}$ is given by

$$f(s; e^{-\bar{\tau}s}) = \alpha s^2 + s + (k_p s + k_i)e^{-\bar{\tau}s} = 0, \tag{37}$$

from which, as per Rule 1, stability condition of the delay-free system can be found as $k_p + 1 > 0$ and $k_i > 0$. Next, one calculates Eqs. (23)–(24), which are found as

$$k_i = -\frac{\omega^*(\alpha\omega^*(\phi^2 - 1) - 2\phi)}{1 + \phi^2}, \tag{38}$$

$$k_p = \frac{2\alpha\omega^*\phi + \phi^2 - 1}{1 + \phi^2}. \tag{39}$$

Following the work of [20], we have $m \leq 2$. One should therefore pay attention when studying the closed form expressions in (38)–(39); in case $m = 2$, the computed (k_p, k_i) values should be checked in Corollary 1 to make sure that these values are feasible.

Lemma 8 *The PI gains, if any, that achieve a delay margin $\bar{\tau}$ in the closed-loop system with (37), are upper bounded.*

Proof The proof follows from the fact that ω^* is upper bounded, and that ϕ^2 terms appear in both the numerators and denominators in (38)–(39). □

The above lemma shows a contrast to the scalar case discussed in the previous subsection where we show that the (a, b) parameter settings could be unbounded for a desired delay margin in the system. This is mainly because there exists an interesting interplay between the parameter ϕ and the way the controller as well as the characteristic equation is structured, which eventually determines the power of ϕ in the closed-form expressions of the system parameters. This ultimately determines the boundedness of these parameters for ever achieving a certain delay margin in the system.

4 Computations

4.1 Example 1

Take the characteristic equation studied in [45]:

$$f(s; e^{-s\bar{\tau}}) = s^3 + e^{-s\bar{\tau}}((\alpha+\beta)(s^2+s)+\beta) = 0, \quad (40)$$

where α and β are design parameters. As per Rule 1, we find out using Routh-Hurwitz stability criterion that the delay-free system is stable if and only if the following conditions hold concurrently:

- $\beta > 0$,
- $\alpha + \beta > 0$,
- $(\beta+\alpha)^2 - \beta > 0$.

Following the approach described above, we obtain α and β as follows

$$\alpha = \frac{(\omega^*)^2}{1+\phi^2}(((\omega^*)^2-1)(\phi^2-1)+2\phi\omega^*), \quad (41)$$

$$\beta = -\frac{(\omega^*)^3}{1+\phi^2}(2\phi+\omega^*(\phi^2-1)). \quad (42)$$

Moreover, (42) can be simplified as

$$\beta = (\omega^*)^2\frac{1-\phi^2}{1+\phi^2} - \alpha, \quad (43)$$

which we present here to also correct the missing $(\omega^*)^2$ typo in the cited study.[6]

One key observation here is that, since the feasible ω^* solution is always upper and lower bounded with respect to ϕ, and since ϕ^2 term appears both in the numerator and denominator of (41)–(42), admissible α and β control gains can be large, if they exist, but will have to be upper bounded for a given $\bar{\tau}$.

Using (41)–(42), we then compute (α, β) pairs for different values of $\bar{\tau}$. Next, one should check whether or not these pairs violate the conditions in Corollary 1. Alternatively, here we check whether or not the TRACE-DDE software [46] confirms the validity of these pairs. Using this software, it is found that no violations occur, and hence the computed pairs are feasible, see Fig. 3. In the figure, we observe that, as the delay margin $\bar{\tau}$ of the system is increased, the feasible (α, β) gain values become smaller, in one sense to accommodate system's stability for larger delays using weaker gains. We also notice that β values reduce much more dramatically compared to α values. Moreover, for (α, β) in the box $[0, 0.5] \times [0, 0.5]$, we see that iso-contours become too close to each other, showing significant sensitivity increase in system's delay margin against variations in (α, β) values. We also observe that smaller values of (α, β) gains do not necessarily mean that system's delay margin will increase, which is contrary to the common sense.

[6] The computational results in the cited study are correct as they were based on (41)–(42).

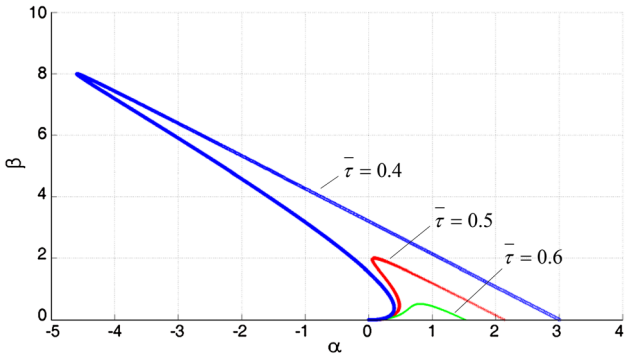

Fig. 3 The parametric settings for (α, β) pairs such that the characteristic equation in (40) has a delay *margin* of $\bar{\tau}$

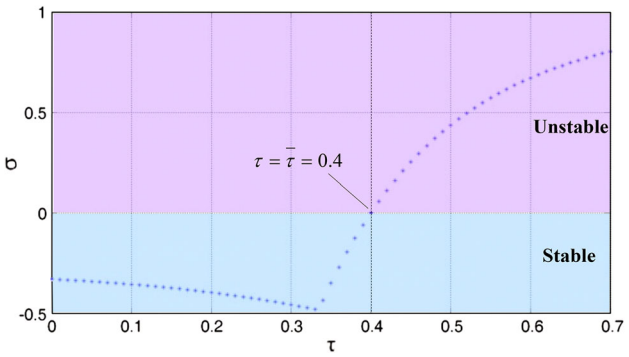

Fig. 4 Given $\bar{\tau} = 0.4$ and the point $(\alpha, \beta) = (-0.7504, 4.001)$ from Fig. 3, the real part σ of the *rightmost root* of the system with the characteristic equation in (40) for a range of delay values τ. Computation was performed using TRACE-DDE software [46]

We next pick a point $P(x, y) = (-0.7504, 4.001)$ on the contour $\bar{\tau} = 0.4$, and compute the rightmost root behavior of the system using TRACE-DDE software [46]. For computations, we sweep the delay value τ from zero to 0.7, and plot the real part σ of the rightmost root of the system, Fig. 4. As expected, we find out that $\sigma < 0, \forall \tau \in [0, \bar{\tau})$, and the system transitions to instability precisely at $\tau = \bar{\tau}$.

4.2 Example 2

Let us study the system with the characteristic Eq. (37). In order to compare the results with those in [30], we first set $\alpha = 4$, $\bar{\tau} = 1$, and obtain the iso-parametric curve in PI controller gain space, as depicted in Fig. 5a. It is easy to verify that the boundary found here is identical to the boundary found in the cited study. However, note that, besides the mathematical approaches being completely different, the study in [30] is concerned with finding the "regions" in the PI gain space where the particular closed-loop system remains stable for a given delay, while the effort here is to compute

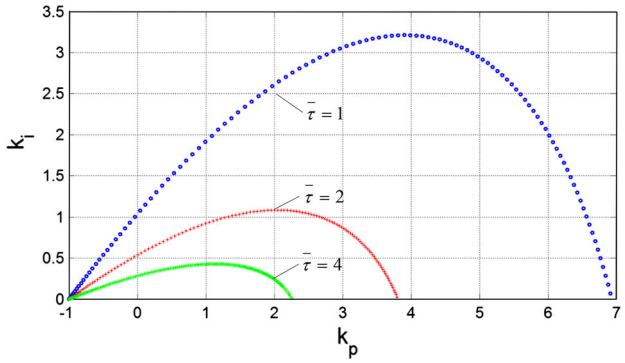

(a) Iso-parameter curve in (k_p, k_i) controller gain space corresponding to the closed-loop system considered in Example 2. Open-loop system time constant is $\alpha = 4$.

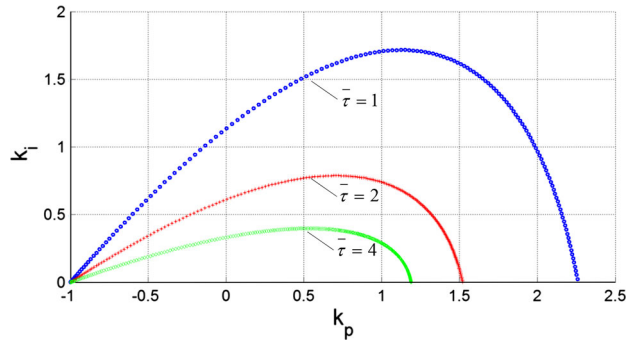

(b) Iso-parameter curve in (k_p, k_i) controller gain space corresponding to the closed-loop system considered in Example 2. Open-loop system time constant is $\alpha = 1$

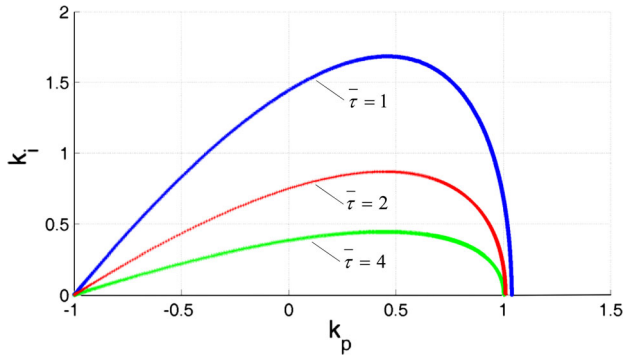

(c) Iso-parameter curve in (k_p, k_i) controller gain space corresponding to the closed-loop system considered in Example 2. Open-loop system time constant is $\alpha = 0.1$

Fig. 5 Example 2: Given the delay margin $\bar{\tau}$, the iso-PI gains are studied for the system described by the characteristic equation in (37).

the particular iso-parametric curves that precisely place the rightmost eigenvalues of system (1) on the imaginary axis for a given delay, while guaranteeing that the system has a delay margin $\bar{\tau}$.

We move forward with additional parametric studies. In particular, we are interested in how the iso-parameter curves change with respect to a, which is inversely proportional to the open-loop-plant bandwidth $1/a$. For this, we investigate combinatorically $\alpha = 4$, $\alpha = 1$, and $\alpha = 0.1$ values with respect to the delay values $\bar{\tau} = 1$, $\bar{\tau} = 2$, and $\bar{\tau} = 4$. The iso-parameter curves are shown in Fig. 5. In this figure, firstly, we observe that, as the bandwidth of the system increases, that is, when α becomes smaller, then the PI controller gains must be reduced in order to maintain the same delay margin in the closed-loop system. Moreover, when the stabilizing PI gains are set in the vicinity of $k_p = -1$ and $k_i = 0$, i.e., the delay-free closed-loop system poles are stable but they are near the imaginary axis of the complex plane, then we observe that all the contours merge into each other, showing that controller parameter space becomes extremely sensitive to small variations, which, in the case of modeling uncertainties, could destabilize the system.

Sensitivity problems arise also in the case of $\alpha = 0.1$, when k_p is selected in the vicinity of $k_p = 1$. Based on the geometric shapes observed in these figures, and/or using the closed-form expressions of k_p and k_i gains, we can also study and judge the parametric space where such sensitivity issues are less dramatic, and less likely to be an issue. For instance, for $\alpha = 4$, in order to achieve a delay margin of $\bar{\tau} = 1$, it makes more sense to select $k_p = 5$ and $k_i \approx 2.9$, instead of choosing $k_p = -0.9$ and $k_i \approx 0.1$, showing interestingly that larger gains can be more feasible for the robust operation of the closed-loop system.

4.3 Example 3

Consider the following state space representation of a system with a second-order open-loop plant described by ω_n and ζ as respectively the natural frequency and damping ratio, and controlled by a PD controller with controller gains $k_p = 10$, and $k_d = 5$, which is influenced by state measurement delay τ,

$$\frac{d}{dt}x(t) = \begin{pmatrix} 0 & 1 \\ -\omega_n^2 & -2\zeta\omega_n \end{pmatrix} x(t) + \alpha \begin{pmatrix} 0 & 0 \\ -10 & -5 \end{pmatrix} x(t-\tau), \tag{44}$$

where $\tau = \bar{\tau}$ is fixed, and one wishes to design the gain α such that the closed-loop system has a delay margin of $\bar{\tau}$.

Following the discussions in Sect. 3.1.1, we obtain two solutions for α, one is denoted by α_1 and the other is α_2, solved respectively from the equations corresponding to (18) and (19),

$$\alpha_1 = \frac{(\omega^*)^2 + 2\zeta\omega_n\phi\omega^* - \omega_n^2}{5(\omega^*\phi + 2)}, \tag{45}$$

$$\alpha_2 = \frac{(\omega^*)^2\phi - 2\zeta\omega_n\omega^* - \phi\omega_n^2}{5(\omega^* - 2\phi)}. \tag{46}$$

Next we explore the case when $\omega_n = 2$, $\zeta = 0.8$, and $\bar{\tau} = 0.1$. Using these numerical values, we form the error function as defined in (20), which reads

$$e(\phi) := \alpha_1 - \alpha_2. \tag{47}$$

One next studies the zeros of the error function, and as explained above, this can be done by sweeping the single parameter ϕ and graphically studying the curve $e(\phi)$. We find out that $\phi = \phi_0 = 1.076841135$ is the only candidate solution of the error function, and although another solution $\phi_1 < 0$ also exists, this solution violates Rule 1, and is thus ignored. Corresponding α solution is calculated as $\alpha = 3.2793$, which is also found to guarantee the stability of the delay-free system, confirming that Rule 1 is satisfied. Moreover, we find, using (14) and $\bar{\tau}$ that $\omega^* = 16.4476$, which complies with Rule 2. Moreover, to be consistent with the conditions in Corollary 1, we perform rightmost root computations using the TRACE-DDE software [46], which confirms that $\alpha = 3.2793$ is the feasible solution.

The next question we wish to answer is how α needs to be adjusted to maintain a certain delay margin in the system, for different values of ω_n and ζ. For this, we pick three different ω_n and ζ values, as reported on Table 1. Moreover, we fix $\bar{\tau} = 0.5$. In this case, α is calculated for each combination of ω_n and ζ while checking compliance with Rule 1-2. Moreover, to be consistent with the conditions in Corollary 1, we again utilize TRACE-DDE software as above, see Table 1 for the results. On the table, we present two different cases, one in which feasible α exists, and the other where a feasible α was not found and thus the corresponding setting is marked with "not applicable N/A". Also, although a generalization is not possible, inspecting Table 1, we see that a larger α value can be used to scale up the PD controller gains in order to keep the same delay margin in the closed-loop system, if either ζ is larger, or ω_n is larger.

Table 1 Example 3. The settings that render the closed-loop system in (44) marginally stable for the delay value $\bar{\tau} = 0.5$, and stable for $0 \leq \tau < \bar{\tau} = 0.5$

ω_n	ζ	α	ω^*
1	0.4	0.3556	2.5206
1	0.7	0.4872	2.9350
1	0.9	0.5652	3.1428
10	0.4	2.0263	7.1514
10	0.7	3.0977	6.7518
10	0.9	3.8177	6.5850
100	0.4	N/A	N/A
100	0.7	N/A	N/A
100	0.9	N/A	N/A

5 Conclusion

An approach for the reverse problem of revealing the iso-delay margin contours in the system parameter and/or controller parameter space of the general single-delay retarded-type LTI system is presented. With this approach, not only one obtains the iso-parameter curves that create the same delay margin in the system, but one can also stabilize such systems, simply by knowing the delay $\tilde{\tau}$ in the closed-loop system, and then selecting $\bar{\tau}$ such that $\bar{\tau} > \tilde{\tau}$ in order to calculate the parameters corresponding to a delay margin of $\bar{\tau}$, which will ultimately guarantee for the same set of parameters that the system is stable at the delay value $\tilde{\tau}$. Extensions of this work to neutral class and fractional type LTI systems can be established by considering additional features of such systems published in the literature.

Acknowledgments The author would like to thank Wei Qiao and Adrián Ramírez for their careful proof reading of the numerical examples in this manuscript.

References

1. Erneux T (2009) Applied delay differential equations. In: Surveys and tutorials in the applied mathematical sciences, vol. 3, Springer, New York
2. Insperger T, Stépán G (2011) Semi-discretization method for time-delay systems. Springer, New York
3. Insperger T, Milton J, Stépán G (2013) "Acceleration feedback improves balancing against reflex delay", J Royal Soc Interface, 10(79):20120763
4. Michiels W, Niculescu S.-I (2007) Stability and stabilization of time-delay systems: an eigenvalue based approach. In: Advances in design and control 12, SIAM Publications, Philadelphia
5. Sipahi R, Niculescu S-I, Abdallah CT, Michiels W, Gu K (2011) Stability and stabilization of systems with time delay, limitations and opportunities. IEEE Control Syst Mag 31(1):38–65
6. Stépán G (2009) (ed), Delay effects in Brain dynamics. Phil. Trans. Royal Soc A, 367,1059–77
7. Zhong Q.-C (2006) Robust control of time-delay systems. Springer, Heidelberg
8. Bellman RE, Cooke KL (1963) Differential-difference equations. Academic Press, New York
9. Datko R (1978) A procedure for determination of the exponential stability of certain differential-difference equations. Q Appl Math 36:279–292
10. Halanay A (1966) Differential equations. stability, oscillations, time lags. Mathematics in Science and Engineering, Academic Press, New York
11. Hale J.K (1977) Theory of functional differential equations. Applied Mathematical Sciences, vol. 3, Springer, New York
12. Popov EP (1962) The dynamics of automatic control systems. Pergamon Press, London
13. Stépán G (1989) Retarded dynamical systems: stability and characteristic function. Longman Scientific & Technical, Wiley, New York
14. Gu K, Kharitonov VL, Chen J (2003) Stability of time-delay systems. Birkhauser, Boston

15. Chen J, Gu G, Nett CN (1995) A new method for computing delay margins for stability of linear delay systems. Syst Control Lett 26(2):107–117
16. Cooke KL, van den Driessche P (1986) On zeros of some transcendental equations. Funkcialaj Ekvacioj 29:77–90
17. Hsu CS, Bhatt KL (1966) Stability charts for second-order dynamical systems with time lag. ASME J Appl Mech 33:119–124
18. Loiusell J (2001) A matrix method for determining the imaginary axis eigenvalues of a delay system. IEEE Trans Autom Control 46(12):2008–2012
19. Olgac N, Sipahi R (2002) An exact method for the stability analysis of time delayed LTI systems. IEEE Trans Autom Control 47:793–797
20. Walton K, Marshall J.E, (1987) "Direct method for TDS stability analysis". IEE Proc, Part D, 134(2):101–107
21. Nia PM, Sipahi R (2013) Controller design for delay-independent stability of linear time-invariant vibration systems with multiple delays. J Sound Vib 332(14):3589–3604
22. Middleton R, Miller D (2007) On the achievable delay margin using LTI control for unstable plants. IEEE Trans Autom Control 52(7):1194–1207
23. Gu K, Niculescu S-I, Chen J (2005) On stability crossing curves for general systems with two delays. J Math Anal Appl 311:231–253
24. Gu K, Naghnaeian M (2011) Stability crossing set for systems with three delays. IEEE Trans Autom Control 56(1):11–26
25. Hale JK, Huang W (1993) Global geometry of the stable regions for two delay differential equations. J Math Anal Appl 178:344–362
26. Jarlebring E (2009) Critical delays and polynomial eigenvalue problems. J Comput Appl Math 224(1):296–306
27. Naghnaeian M, Gu K (2013) Stability crossing set for systems with two scalar-delay channels. Automatica 49(7):2098–2106
28. Sipahi R, Delice II (2011) Advanced clustering with frequency sweeping methodology for the stability analysis of multiple time-delay systems. IEEE Trans Autom Control 56(2):467–472
29. Sipahi R, Olgac N (2005) Complete stability robustness of third-order LTI multiple time-delay systems. Automatica 41(8):1413–1422
30. Silva GJ, Datta A, Bhattacharyya SP (2001) PI stabilization of First-order systems with time delay. Automatica 37:2025–2031
31. Fioravantia AR, Bonnet C, Özbay H, Niculescu S.-I (2012) "A numerical method for stability windows and unstable root-locus calculation for linear fractional time-delay systems". Automatica 48(11):2824–2830
32. Rekasius ZV (1980) "A stability test for systems with delays". Presented at proceedings of the joint automatic control conference, Paper No. TP9-A
33. Delice II, Sipahi R (2012) Delay-independent stability test for systems with multiple time-delays. IEEE Trans Autom Control 57(4):963–972
34. Korogui RH, Fioravanti AR, Geromel JC (2011) On a rational transfer function-based approach to H1 filtering design for time-delay linear systems. IEEE Trans Signal Process 59(3):979–988
35. Münz U, Ebenbauer C, Haag T, Allgöwer F (2009) Stability analysis of time-delay systems with incommensurate delays using positive polynomials. IEEE Trans Autom Control 54(5):1019–1024
36. Souza FO, de Oliveira MC, Palhares RM (2009) Stability independent of delay using rational functions. Automatica 45(9):2128–2133
37. Thowsen A (1982) Delay-independent asymptotic stability of linear systems. IEE Proc. D Control Theory Appl 129(3):73–75
38. Sipahi R, Olgac N (2006) Stability robustness of retarded LTI systems with single delay and exhaustive determination of their Imaginary spectra. SIAM J Control Optim 45(5):1680–1696
39. Niculescu S.-I (2001) Delay effects on stability: a robust control approach. In: Lecture notes in control and information sciences, vol. 269, Springer, Berlin
40. Barnett S (1983) Polynomials and linear control systems. Marcel Dekker, New York
41. Fazelinia H, Sipahi R, Olgac N (2007) "Stability robustness analysis of multiple time-delayed systems using 'building block concept". IEEE Trans Autom Control 52(5):799–810
42. Chen J, Latchman HA (1995) Frequency sweeping tests for asymptotic stability independent of delay. IEEE Trans Autom Control 40(9):1640–1645
43. Sipahi R, Delice II (2009) Extraction of 3D stability switching hypersurfaces of a time delay system with multiple fixed delays. Automatica 45(6):1449–1454
44. Gelfand I.M, Kapranov M.M. Zelevinsky A.V (1994) Discriminants, resultants, and multidimensional determinants. Ser. Mathematics: Theory & Applications. Birkhäuser, Boston
45. Sipahi R "Model-free approach to controlling nonlinear systems with single output delay". In: American control conference, pp. 3913–3918, Montreal, 27–29 June 2012
46. Breda D, Maset S, Vermiglio R (2006) Pseudospectral differencing methods for characteristic roots of delay differential equations. SIAM J Sci Comput 27:482–495